Available online at www.eccomasproceedia.org
Eccomas Proceedia COMPDYN (2021) 2421-2434

ECCOMAS
Proceedia

COMPDYN 2021
8th ECCOMAS Thematic Conference on
Computational Methods in Structural Dynamics and Earthquake Engineering
M. Papadrakakis, M. Fragiadakis (eds.)
Streamed from Athens, Greece, 28 - 30 June 2021

SEISMIC RISK ASSESSMENT OF ROCKING BUILDING CONTENTS

Michalis Fragiadakis[1], **Spyridon Diamantopoulos**[1]

[1] School of Civil Enginnering, National Technical University of Athens
9 Iroon Polytechniou 15780, Zografou Campus, Athens, Greece
e-mail: mfrag@mail.ntua.gr; sdiamadop@central.ntua.gr

Abstract. *The paper presents a fully performance-based seismic reliability and risk assessment framework for freestanding structural components and contents that can be modelled as rocking rigid blocks. It shown that a drift-driven Incremental Dynamic Analysis approach can be adopted in order to obtain the floor timehistories which are then used as input for the response history analysis of the contents. Therefore, first the demand at the storey level is obtained and then the response of the contents is calculated using the storey acceleration response history. An alternative methodology where the fragility of the building and of the freestanding contents are derived separately is also examined and its limitations are discussed. The seismic response of building contents depends on several parameters such as the geometry of the object, the dynamic characteristics of the building and the storey that the object is located.*

Keywords: building contents, Incremental Dynamic Analysis, fragility, nonstructural, rocking, freestanding.

ISSN:2623-3347
Peer-review under responsibility of the organizing committee of COMPDYN 2021.
doi:10.7712/120121.8647.20536

1 INTRODUCTION

Earthquake losses may be due to structural damage, damage of non-structural components (e.g. infills, piping system) and also due to the damage of the structure's contents. Non-structural damage can be due to damage of components attached, or anchored, to the hosting building, or due to damage on the freestanding inventory of the building. In the latter case, there is a huge variability of systems and configurations hampering the systematic study of the problem and the recommendation of generally-applicable guidelines. The risk assessment of building contents is a complicated task since the response of the contents depends also on the behaviour of the hosting structure. As a result, there may be cases where a strong earthquake does not overturn an object but strongly damages the structure, while more benign ground motions may leave the structure intact however causing losses due to damage on the building's contents.

The paper focuses on the seismic performance, fragility and risk assessment of freestanding building contents. Freestanding building contents are treated as rocking rigid blocks and are modelled using Housner's theory [1]. A specifically tailored version of the Incremental Dynamic Analysis (IDA) method is proposed in order to assess the structure and its contents considering that the structural collapse implies also collapse/overturning of the contents [2]. A second point of interest is the derivation of fragility curves and the calculation of the Mean Annual Frequency (MAF) of building contents.

Despite the significance of the problem, there are relatively few past studies on the seismic response assessment of freestanding contents, especially compared to the case of anchored non-structural components and anchored building equipment. The paper presents a performance-based seismic fragility and risk assessment framework for freestanding building contents. Contrary to previous works on the seismic fragility assessment of rocking contents, the proposed methodology discusses how the response of the hosting building and that of the contents are coupled and also the effect of different stories and different block geometries. In order to consistently study the effect of increasing seismic intensity in a performance-based setting, a modified version of the well-known Incremental Dynamic Analysis (IDA) method is presented. It is shown that the EDP that should "drive" the IDA simulations is that of the building rather than that of the contents and also that the collapse of the building should not be neglected. Moreover, the calculation of fragility and risk are discussed. Existing fragility assessment methodologies are adopted showing that the IM of the building should be adopted (instead of that of the contents), while a procedure that uses the total probability theorem in order to calculate the MAFs combining fragilities that were separately generated for the structure and for the contents is investigated. Overall it is shown that the problem is not as simple, as it may initially seem, and that various tools should be appropriately combined in order to accurate and efficiently calculate the risk of freestanding contents.

2 Theory of the rocking block

In order to study the seismic response of freestanding bodies to an earthquake ground motion, it is assumed that the bodies are orthogonal blocks. Following the pioneering work of Housner [1], the problem of rocking and overturning of freestanding blocks to earthquakes has been the subject of intense analytical and experimental research. Despite its apparent simplicity, the rocking problem has been proven difficult, since the blocks behave nonlinearly and also due to the occurrence of many impacts between the rocking bodies and their base. The fundamentals of rocking theory are briefly summarized in order to allow studying the seismic behaviour of

freestanding rocking blocks. A rigid block of dimensions $2b \times 2h$ that oscillates about pivot point A (or A'). The block has weight W and moment of inertia I_0 about point A.Assuming that the block is homogeneous and thus the center of gravity is located at height h, the block's slenderness angle is equal to $\alpha = atan(b/h)$. The slenderness angle α together with the size parameter $R = \sqrt{b^2 + h^2}$ define fully the geometry of the block. Consequently, the equation of motion of the rocking block is [1]:

$$I_o\ddot{\theta}\left(t\right) + mgR\sin\left[\alpha\mathrm{sgn}\theta\left(t\right) - \theta\left(t\right)\right] = -m\ddot{u}_g\left(t\right)R\cos\left[\alpha\mathrm{sgn}\theta\left(t\right) - \theta\left(t\right)\right] \quad (1)$$

where the angle of rotation θ is the only degree of freedom. The sign function is used to define the pivot point (A or A'), i.e. when A' is the pivot point, the angle θ is negative. The above Eq. 1 can be solved either with the aid of an Ordinary Differential Equation (ODE) solver or using simple Finite Element models (e.g Diamantopoulos and Fragiadakis[3]).

3 Seismic response assessment of building contents

The procedure followed for the seismic response assessment of freestanding building contents is relatively easy. The building is subjected to an acceleration timehistory and the total acceleration response history of the storey of interest is stored. The stored storey acceleration response history is used as the input acceleration time history for the rigid block assessment. This conceptually simple cascading procedure requires two models, one for simulating the building and a second for simulating the freestanding contents. Moreover, after every building simulation the complete acceleration, or velocity, response history has to be stored for every storey. This workflow is used also for developing the fragility curves of the rocking objects of interest.

Seismic response assessment requires to define pertinent Intensity Measures (IM) and Engineering Demand Parameters (EDP) for both the structure and the contents. This step is also important for the fragility assessment. IMs represent seismic intensity, while the EDPs are used to measure the demand, or the "damage". In order to distinguish the quantities that refer to the "structure" and the "block', the superscripts "s" and "b" ' are used, respectively. Therefore, $EDP^{(s)}$ and $IM^{(s)}$ are the IM and the EDP of the structure, while $EDP^{(b)}$ and $IM^{(b)}$ refer to the rigid block. For a block at storey j, $IM^{(b)}$ will coincide with (or be derived from) the structure's $EDP_j^{(s)}$, or, simply, the peak floor acceleration of the storey is the peak ground acceleration for the rocking body. Therefore, the selection of $EDP_j^{(s)}$ and $IM^{(b)}$ should be consistent.

For moderate-period structures with no near-fault activity, an appropriate choice for the intensity measure of the building $IM^{(s)}$, is the 5%-damped, first-mode spectral acceleration, $S_a(T_1, 5\%)$. Moreover, the most common EDP for moment frames is the maximum interstorey drift. However, since our focus is on freestanding components, instead of the maximum interstorey drift, a consistent quantity should be chosen as the $EDP^{(s)}$, while the intensity measure $IM^{(s)}$ is always $S_a(T_1, 5\%)$, although other measures are also possible.

For a rocking block, the most intuitive IM choice is the peak ground acceleration (PGA), since it is the parameter that defines the maximum overturning moment, while according to $\ddot{u_g} \geq \tan\alpha$ and $\ddot{u_g} \geq \mu\tan\alpha$ the PGA defines whether rocking and sliding respectively or none of the two will occur. Although it is not necessary, the PGA is normalized with $gtan\alpha$ and thus the block's IM is $IM^{(b)} = PGA/gtan\alpha$, where $IM^{(b)} \leq 1$ implies that the block does not start rocking. Furthermore, past research[4, 5] has shown that the PGV is also an important response parameter that provides a good correlation between seismic demand and block overturning. For simplicity, we choose not to normalize the PGV, but researchers[**?**] have

also proposed the normalized quantity $pPGV/gtan\alpha$ as an IM suitable for rocking blocks. Our results have shown that the PGV (or PFV) performs well as an IM and hence we have chosen the simplest IM possible. Therefore, the $IM^{(b)}$ for a rocking block at storey j considered, is either the normalized peak floor acceleration PFA_j, or the peak floor velocity PFV_j; the parameter chosen will be also used as the demand parameter of the building $EDP_j^{(s)}$. The most suitable engineering demand parameter $EDP^{(b)}$ for the rocking block is the rotation angle θ normalized by slenderness angle α, i.e. $EDP^{(b)} = |\theta|/\alpha$.

In order to assess a system's capacity, meaningful performance objectives related with the system's modes of failure or damage have to be identified. For rocking systems, overturning is the primary limit-state of interest, while rocking initiation is also of interest but it can be easily identified from the PGA. Depending on the freestanding component, (e.g. its purpose, its material, etc), "limited" damage can be identified for normalized rotation values $\theta/\alpha \approx 0.1 \div 0.3$, "moderate" damage for $\theta/\alpha \approx 0.3 \div 0.5$ and "overturning" is assumed for $\theta/\alpha \geq 1$. Recommendations of limit-state thresholds for rocking bodies can be found in various publications, e.g. Dimitrakopoulos and Paraskeya[6], Psycharis *et al.*[7] and Kavvadias *et al.*[8]. In practice, these limits vary considerably and it is not possible to decide threshold values that are generally applicable. For example, for sensitive mechanical equipment a rotation $\theta/\alpha \geq 0.1$ may result to permanent damage and thus in terms of loss the outcome will be the same with overturning. Another important aspect is the geometry of the block. Slender blocks start rocking for smaller acceleration values, while stocky blocks require higher acceleration values to start rocking and are more stable.

4 Fragility and risk calculations

The seismic risk assessment of building contents requires the prior knowledge of their fragility. As fragility, or "fragility function", we refer to the cumulative distribution function of the capacity of an asset to resist an undesirable limit-state [9]. For building contents, the fragility provides the probability of overturning as a function of the seismic excitation. Although often in the literature the terms "fragility" and "vulnerability" are used interchangeably, in this work we assume that fragility refers to the overturning probability as function of seismic intensity, while vulnerability is used to measure loss. Past research on fragility assessment focuses on the risk assessment of the structure itself[10], while the contents are examined separately and, usually, neglecting the effect of the hosting structure. Independent, and often generic, fragility curves for various building contents can be found in guidelines (e.g. FEMA P-58[11]) and the literature. Such fragility curves are empirical and are targeted to specific component types (e.g. cladding panels, masonry parapets). The direct fragility calculation that is here proposed through simulations allows to consider additional sources of uncertainty (e.g. related to the shape of the object, its mass distribution) and hence is preferable.

The fragility function is the conditional limit-state exceedance probability, given by the expression:

$$F_R = P(EDP > edp|IM) \tag{2}$$

The structure is first examined. There will be simulations that the building collapses (denoted as "C") and simulations where no collapse occurs (denoted as "NC"). Making this separation and dropping the conditioning term in order to simplify the notation, i.e.: $P(EDP) = P(EDP > edp|IM)$, the probability of Eq. 2 is calculated using the total probability theorem (TPT) as follows:

$$F_R^{(s)} = P(EDP^{(s)}|NC)P_{NC} + P(EDP^{(s)}|C)P_C \Leftrightarrow$$

$$F_R^{(s)} = P(EDP^{(s)}|NC)(1 - P_C) + P_C \tag{3}$$

where $P(EDP > edp^{(s)}|C)$ is equal to 1 since the inequality is always satisfied and $P_{NC} = 1 - P_C$.

Focusing on the rocking body, when an object is subjected to a seismic ground motion there are three possible types of response: (i) the object may not rock and remain at rest, (ii) it may rock, or (iii) it may overturn. Using the total probability theorem for the block, the fragility function becomes:

$$F_R^{(b)} = P(EDP^{(b)}|NoRock)P_{NoRock} + P(EDP^{(b)}|Rocking)P_{Rocking} + P(EDP^{(b)}|Ovtn)P_{Ovtn} \tag{4}$$

where $P(EDP^{(b)}|NoRock)$, $P(EDP^{(b)}|Rocking)$ and $P(EDP^{(b)}|Ovtn)$ are the probabilities that $EDP^{(b)} = \theta/\alpha$ exceeds a threshold value $edp^{(b)}$ and P_{NoRock}, $P_{Rocking}$ and P_{Ovtn} are the corresponding probabilities of no rocking, rocking and overturning, respectively. Blocks that will not rock, will not exceed any $edp^{(b)}$ value and thus $P(EDP|NoRock) = 0$, while the overturning blocks always exceed the limit-state threshold and thus $P(EDP|Ovtn) = 1$. The conditional limit-state probability (fragility) is further simplified to:

$$F_R^{(b)} = P(EDP^{(b)} \geq edp|Rocking)(1 - P_{Ovtn} - P_{NoRock}) + P_{Ovtn} \tag{5}$$

The calculation of Eq. 5 is discussed in the sections that follow. A fundamental assumption of our derivation is that *the simulations that collapse the building also overturn/collapse the freestanding contents* [2].

The risk is expressed as the mean annual frequency (MAF) of a limit-state being exceeded. Adopting the PEER's formula, the limit-state MAF for the structure and for a rigid block are calculated with the aid of the following expressions: where $\lambda_{EDP}^{(s)}$, $\lambda_{EDP}^{(b)}$ is the mean annual frequency of the engineering demand parameter ($EDP^{(s)}$ or $EDP^{(b)}$) exceeding threshold level and $d\lambda_{IM}^{(s)}$, $d\lambda_{IM}^{(b)}$ is the slope of the seismic hazard curve. The limit-state MAFs are easily obtained convolving the site hazard curve, expressed as function of the IM, with the fragility curve obtained with respect to any of the EDPs of interest. For the structure, the IM of interest is always available, e.g. spectral acceleration $S_a(T_1, 5\%)$, but for the block this information is available only at the ground floor. For assets located at a storey, the calculation of $d\lambda_{IM}^{(b)}$ has no meaning and thus their fragility should be calculated as function of $IM^{(s)}$ instead of $IM^{(b)}$:

$$\lambda_{EDP}^{(b)} = \int_{IM^{(s)}} P(EDP^{(b)}|IM^{(s)}) \, |d\lambda_{IM}| \tag{6}$$

Conditioning the block's fragility to $IM^{(s)}$, i.e. using Eq. 6 is also conceptually preferable since the MAF is directly calculated from the site's hazard. Note that we have dropped the superscript "s" from $d\lambda_{IM^{(s)}}$, since $d\lambda_{IM}$ always refers to the site and thus the structure.

A simplified and more generic methodology for the seismic risk of structure's contents is possible if we apply the total probability theorem (TPT), using the block's intensity measure $IM^{(b)}$ as an intermediate variable. This allows to expand Eq. 6 and obtain the MAF using the expression:

$$\lambda_{EDP}^{(b)} = \int_{IM^{(s)}} \int_{IM^{(b)}} P(EDP^{(b)}|IM^{(b)}) \, dP(IM^{(b)}|IM^{(s)}) \, |d\lambda_{IM}| \tag{7}$$

where $P(IM^{(b)}|IM^{(s)}) = P(EDP^{(s)}|IM^{(s)})$ is the building's fragility curve. Eq. 7 can be used in order to calculate separately the fragilities thus bypassing the need for performing building simulations and storing the response acceleration histories for the stories of interest.

5 Incremental Dynamic Analysis for freestanding components

The Incremental Dynamic Analysis (IDA) method is used for calculating the limit-state fragilities for both the structure and its contents. IDA involves subjecting the structure, or the block, to a suite of ground motion records, each scaled to multiple levels of intensity. After incrementally scaling every ground motion, single record capacity curves are produced in terms of demand versus seismic intensity.IDA has conceptual similarities to the Multiple Stripe Analysis (MSA) method[12, 13], where instead of scaling separately all ground motions, every record is scaled to the same IM level. Since for every scaling level the ground motions have the same IM value, the EDP values form a "stripe" which allows to directly calculate the median (50% percentile) and the 16% and 84% percentile capacity curves conditional on the IM. Strictly speaking, in IDA the scaling factors will be different, but stripped data can be easily obtained with interpolation. For the sake of simplicity, in this work MSA was performed (i.e. scaling the records to a common IM level), but loosely speaking the "term" IDA is used since it is more widespread and difference is merely a matter of implementation. Below we first discuss how the IDA method is applied for the cascading problem at hand. We first examine the structure since the ground motions are applied at the base of the building and in the subsection that follows we discuss how the fragilities of the freestanding contents are obtained from the floor response histories.

5.1 Hosting structure

For the four-storey RC building considered [2], every IDA curve is plotted in the EDP-IM plane as shown in Figure 1. The median curve (50% percentile) provides an estimate of the expected value and the fractile curves can be used to measure the dispersion[14]. The IDA capacity curve of Figure 1 is not the most common form of IDA where $EDP^{(s)}$ is the maximum interstorey drift ratio. A different EDP has to be adopted for studying building contents which leads to the representation of Figure 1, where the $EDP^{(s)}$ is either the normalised peak floor acceleration (PFA), or the peak floor velocity (PFV). The summarized EDP-IM plots (Fig. 1a or b) allow to directly calculate $P(EDP_j^{(s)}|NC)$ and P_C (Eq. 3) for every IM stripe. If the $EDP_j^{(s)}$ values are lognormally distributed, the buildings fragility for the j^{th} storey is calculated as follows:

$$P(EDP^{(s)} \geq edp^{(s)}) = 1 - P(EDP^{(s)} < edp^{(s)}) = \Phi\left(\frac{\mu_{logEDP} - edp^{(s)}}{\sigma_{logEDP}}\right) \tag{8}$$

where μ_{logEDP} and σ_{logEDP} are the mean and the standard deviation of the logarithm of the demand, always conditional on the $IM^{(s)}$. Regardless the IM, the fragility of the building should be obtained combing Eq. 8 with Eq. 3:

$$F_R^{(s)} = \Phi\left(\frac{\mu_{logEDP} - edp^{(s)}}{\sigma_{logEDP}}\right)(1 - P_C) + P_C \tag{9}$$

where P_C is the percentage of collapsed simulations. Obviously different fragilities will be obtained depending on the EDP of interest.

Based on Figure 1 and Eq. 8 it is understood that the calculation of Eq. 8 is not efficient when the drift is used as the EDP. This is understood looking at Figure 1 where it is evident that the median (or the 16, 84% fractile) curves, conditional on the IM, cannot be calculated above the IM level where more than 50% (or the 16, 84% fractile, respectively) of the single-record

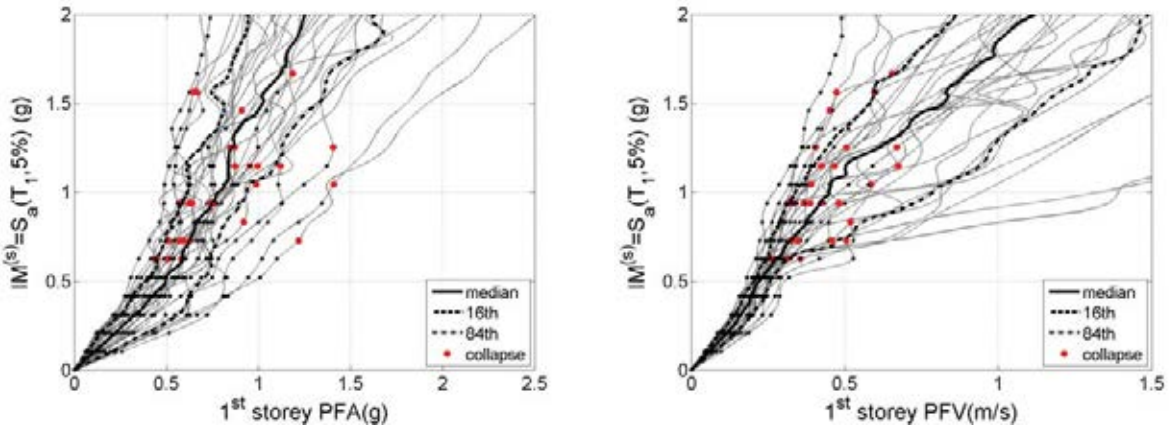

(a) (b)

Figure 1: Storey capacity curves for the four-storey RC building considered, using as EDP: (a) the Peak Floor Acceleration (PFA), and (b) the Peak Floor Velocity (PFV).

IDAs become horizontal. On the contrary, when the PFA, or the PFV, is adopted, the median and the 16, 84% fractiles can be easily calculated due to the practically monotonic increase of the IDA curves.

Moreover, although the drift is not the primary EDP of interest, the IDAs should be driven by the drift, or any other EDP that is related with the structural damage. This is because when structural collapse occurs, the freestanding contents are also considered collapsed (overturned). In the single-record capacity curves of Figure 1, the solid dots indicate when the building collapses, i.e. either when the analysis structurally fails, or when the maximum drift threshold is exceeded. The dots are transferred in Figure 1 indicating the occurrence of structural failure. This is done merely for visualization purposes since all simulations after the dots are assumed collapsed. This visualization shows that even for relatively low PFA, or PFV values, structural damage may have already occurred.

5.2 Rocking contents

Figure 2 shows the EDP-IM plots of a freestanding block with $R = 1.0m$ and $\alpha = 0.2$. The hosting structure was subjected to the IDA simulations of Figures 1 and 3 and then the simulations (shown as black dots in Fig. 1) are transferred to the $EDP^{(b)} - IM^{(b)}$ (Fig. 2a), or the $EDP^{(b)} - IM^{(s)}$ plane (Fig. 2b). In both plots the collapsed simulations appear as dots just right to the vertical line at $EDP^{(b)} = 1$. The dots below the horizontal line at $IM^{(b)} = 1$ (Fig. 2a) correspond to the no rocking simulations. As already discussed in a previous section, the $EDP^{(b)} - IM^{(b)}$ representation is the natural EDP-IM choice, but is not the easiest choice when it comes to the calculation of MAF $\lambda_{EDP}^{(b)}$. Moreover, as shown in Figure 2a, the data in the $EDP^{(b)} - IM^{(b)}$ form a cloud, while if they are plotted in the $EDP^{(b)} - IM^{(s)}$ place they are already conditional on the $IM^{(s)}$.

Both EDP-IM representations allow to calculate the fragility of the blocks, but with respect to a different IM. Defining the fragility conditional on the IM of the structure, i.e. $F_R^{(b)} = P(EDP^{(b)}|IM^{(s)})$ can be used for directly calculating the MAF using Eq. 6. On the other hand, the intuitive definition $F_R^{(b)} = P(EDP^{(b)}|IM^{(b)})$ provides the storey fragilities with respect to the block's IM and always for the storey of interest. Another major difference is that when $IM^{(b)}$ is adopted, the EDP-IM data appear as a "cloud" (Fig. 2a), while when $IM^{(s)}$

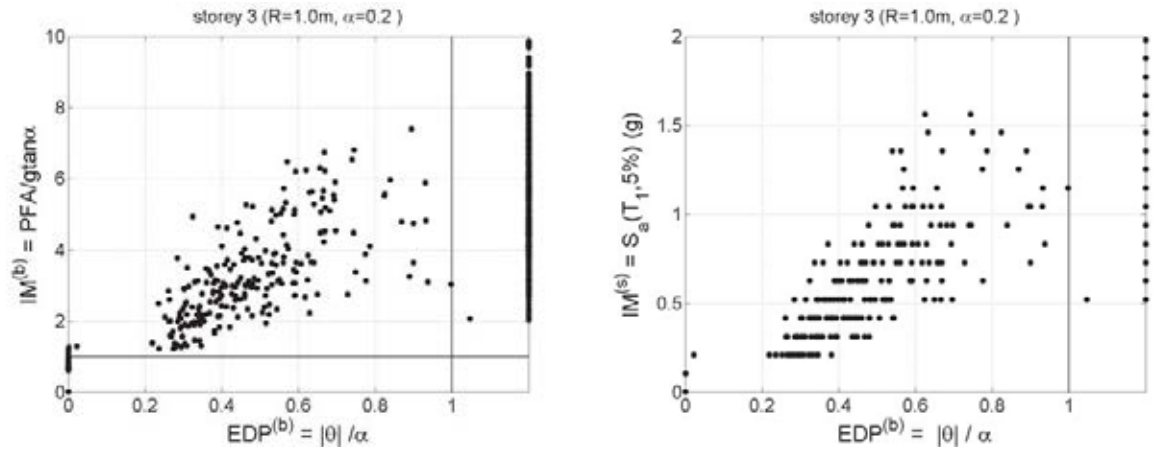

(a) (b)

Figure 2: Seismic response of a freestanding building object with $R = 1.0m$ and $\alpha = 0.2$: (a) plotting $EDP^{(b)} - IM^{(b)}$ results to cloud data, (b) plotting $EDP^{(b)} - IM^{(s)}$ results to data in stripes.

is adopted instead, they appear in stripes (Fig. 2b). The IDA method can be directly applied to the striped data, while the cloud data require a different post-processing in order to derive the fragility curve. In the case of Figure 2b, the data form stripes and hence they can be post processed as was already shown in Section 5.1 for the building:

$$F_R^{(b)} = \Phi\left(\frac{\mu_{logEDPb} - edp^{(b)}}{\sigma_{logEDPb}}\right)(1 - P_{Ovtn} - P_{NoRock}) + P_{Ovtn} \tag{10}$$

Since the $F_R^{(b)}$ is calculated at every stripe P_{NoRock}, P_{Ovtn} are simply obtained as the percentage of simulations where no-rocking and overturning was observed, respectively. An alternative efficient way is to fit the cumulative distribution function (CDF) of a lognormal distribution on the striped EDP-IM data as discussed by Baker [15]. If the data are not stripped, as in Figure 2a, the cloud analysis method should be used instead.

6 Numerical Results

The acceleration and the velocity response spectra [2] allow to understand how the structure filters the record, i.e. they show the modes that are amplified and those that are filtered out. However, rocking structures do not have modes of vibration in the classical sense, i.e. like an elastically deforming body. For this reason, Figure 3 shows the mean rotation demand for two rigid blocks with the same size parameter $R = 1m$ and varying slenderness angle α. A smaller slenderness α value implies a more slender block, hence the block is more sensitive to overturning and keen to larger rotations. Having set overturning simulations to $\theta/\alpha = 1$, very interesting findings are offered by Figure 3. At $S_a(T_1, 5\%)$=0.4g (Fig. 3), the mean rotations of the scaled ground motions are very close to that of the top storey, while the demand is considerably smaller at lower stories. When the building is inelastic ($S_a(T_1, 5\%)$=1.0g, Fig. 3b), the blocks that are subjected to the storey response histories have smaller rotation demand compared to the "ground" records. Therefore, regardless of the $S_a(T_1, 5\%)$ level, the building alters the frequency content of the ground motions reducing the fragility of the block for any slenderness angle α.

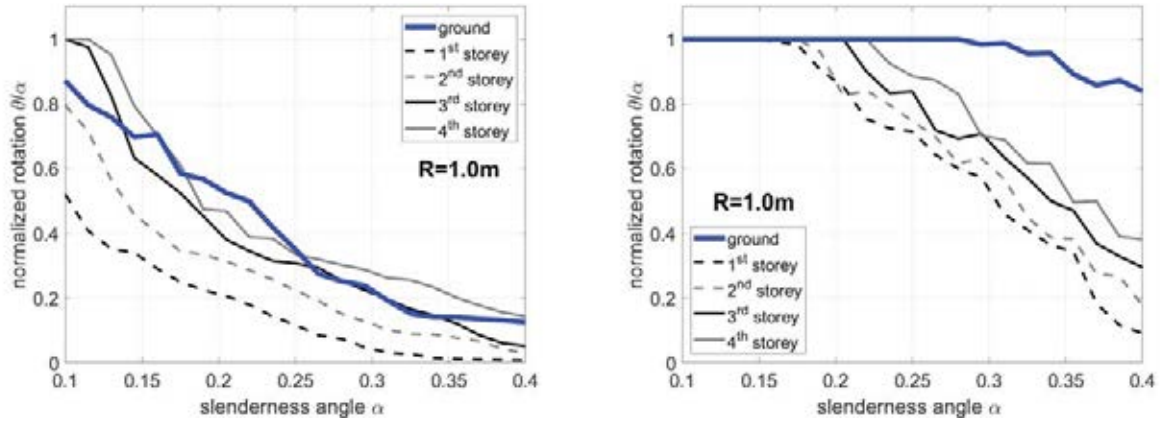

(a) (b)

Figure 3: Mean rotation demands for rigid blocks with $R = 1m$ as function of the slenderness angle. The spectra were produced for building response histories scaled at: (a) $IM^{(s)} = 0.4g$ (elastic structure), and (b) $IM^{(s)} = 1.0g$ (inelastic structure).

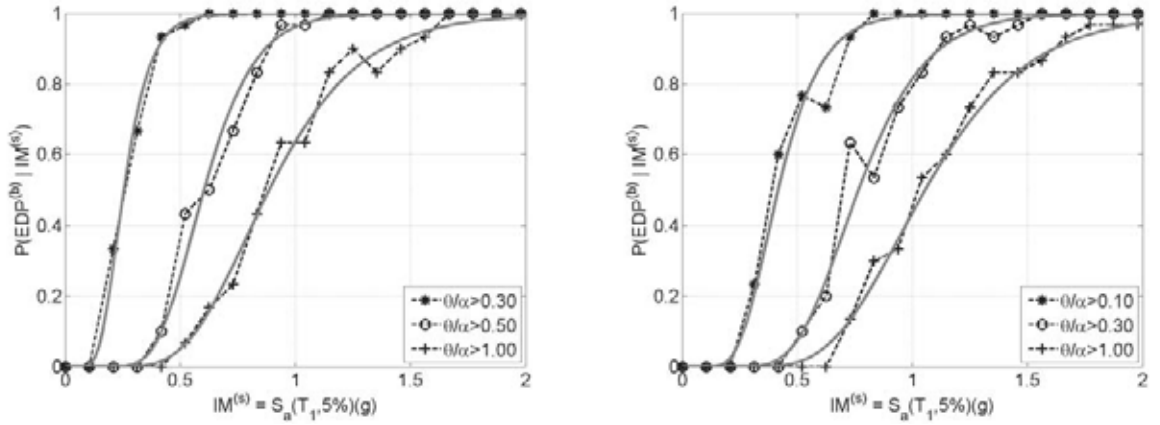

(a) (b)

Figure 4: Fragility curves for a block located at the 3^{rd} storey of the building: (a) slender block ($R = 1.0m, \alpha = 0.2$), (b) stocky block ($R = 1.0m, \alpha = 0.35$).

The remaining of the paper is focused on the seismic fragility assessment of the freestanding contents. We isolate two freestanding rocking blocks with $R = 1m$. The first has a slenderness angle $\alpha = 0.20$ and is considered as "slender", while the second has $\alpha = 0.35$ and is referred as "stocky". Three limit-states are identified for each block. For the slender block, the corresponding $EDP^{(b)} = \theta/\alpha$ threshold values are assumed as 0.3, 0.5 and 1, respectively, while for the stocky block the values are 0.1, 0.3 and 1. Different threshold values are used for each block due to their very different dynamic behaviour (e.g. see Fig 3). For example, $\theta/\alpha = 0.1$ is easily exceeded for the slender block and thus it is not a reasonable threshold, while for a stocky block the limit-state fragility of $\theta/\alpha = 0.5$ will, practically, coincide with that of overturning ($\theta/\alpha \geq 1$).

Figure 5 shows the block overturning fragilities using PFA as the intensity measure $IM^{(b)}$ of the block. The solid lines refer to the block subjected to the original ground motions, while the dashed lines were obtained using the response history of the fourth storey. Also, the dark

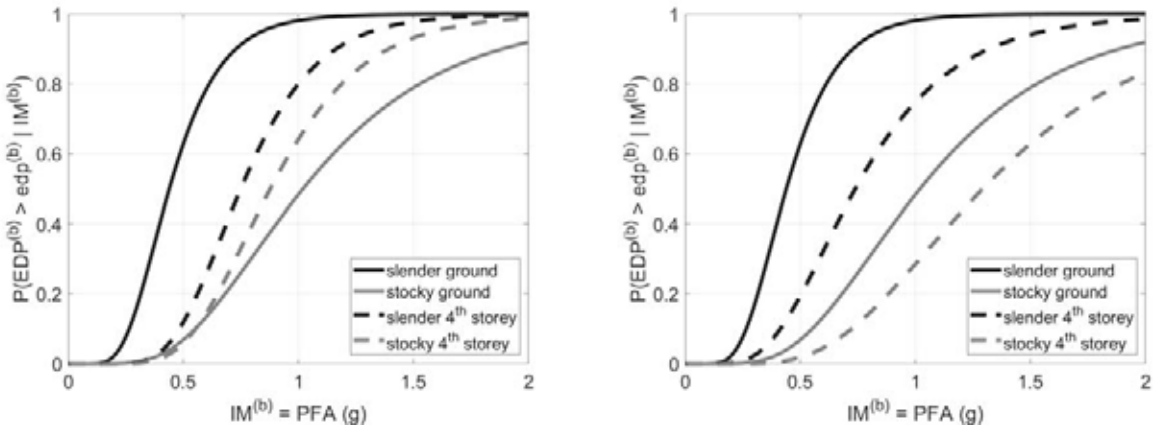

(a) (b)

Figure 5: Overturning fragility curves of a slender ($R = 1.0m$, $\alpha = 0.2$) and a stocky block ($R = 1.0m, \alpha = 0.35$) assuming $IM^{(b)} = PFA$: (a) the block is considered overturned when the structure collapses, (b) the collapse of the structure is omitted.

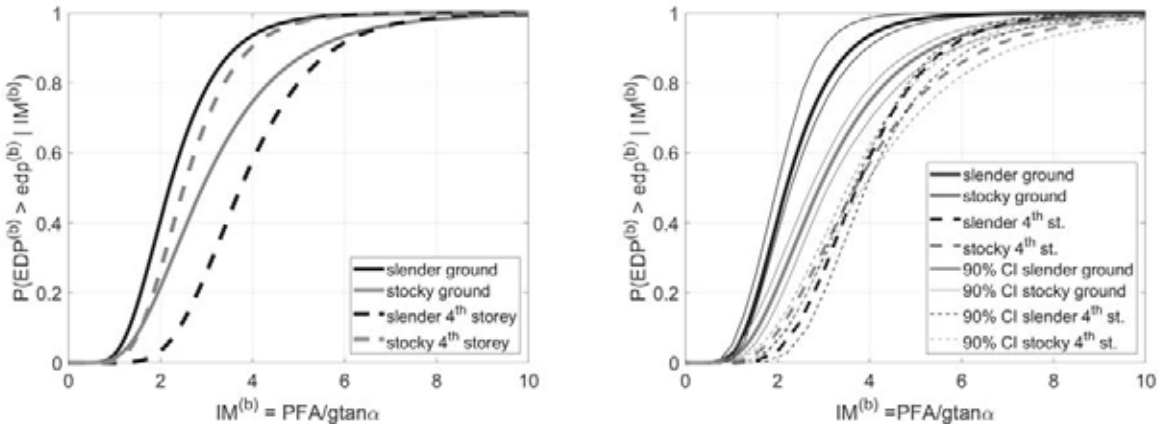

(a) (b)

Figure 6: Overturning fragility curves of a slender ($R = 1.0m$, $\alpha = 0.2$) and a stocky block ($R = 1.0m, \alpha = 0.35$) assuming $IM^{(b)} = PFA/gtan\alpha$: (a) the block is considered overturned when the structure collapses, (b) the collapse of the structure is omitted.

lines correspond to the slender block and the grey to the stocky. As expected, the slender block is always more vulnerable, while the building reduces its fragility (Fig. 5a). On the contrary, the building fragility overall increases for the stocky block. This is in agreement with the rocking spectra of Figure 3. In order to better understand the importance of considering the collapse of the structure, Figure 5b, repeats the fragility curves of Figure 5a, but this time ignoring the coupling between the structure and the block. In other words, in Figure 5b, we do not assume that the block overturns when structural collapse occurs. As before, for the slender block the fragilities are only slightly affected, but for the stocky block the fragility is very different. According to Figure 5a and b, when the coupling is neglected, the building is beneficial also for the stocky block.

The results of Figure 5 are repeated in Figure 6 but with $IM^{(b)} = PFA/gtan\alpha$, instead of PFA. Since the blocks have a different slenderness angle α, the normalized $IM^{(b)}$ affects the

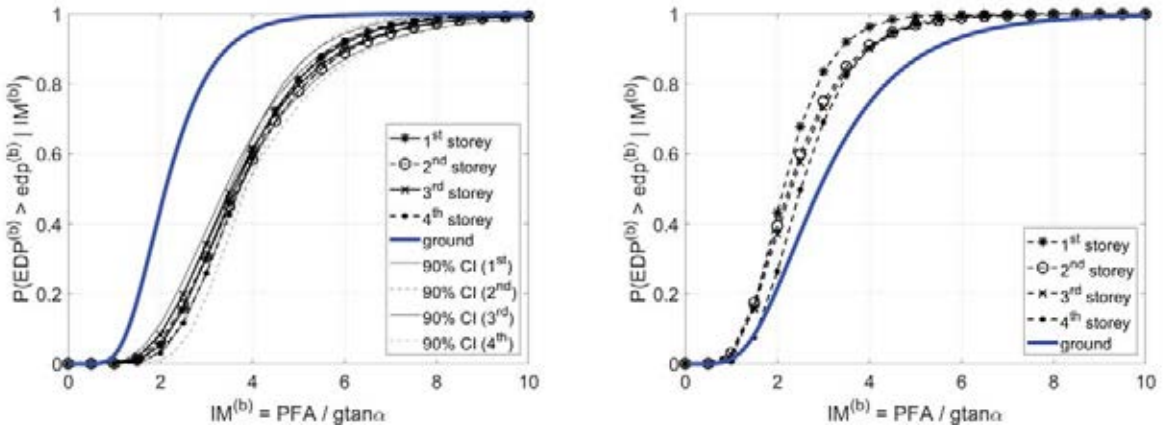

(a) (b)

Figure 7: Storey overturning fragility curves: (a) slender block ($R = 1.0m, \alpha = 0.2$), (b) stocky block ($R = 1.0m, \alpha = 0.35$).

fragilities obtained. Qualitatively the results are the same compared to those of Figure 5a and b, but the fragilities curves are less dispersed, bringing closer the slender and the stocky block fragilities. Figure 6b also shows the 90% bootstrap confidence intervals around each fragility curve. The narrow confidence intervals obtained, verify that the comparison is statistically significant.

Figure 7 presents for all stories of the structure the block overturning fragilities assuming $IM^{(b)} = PGA/gtan\alpha$. For both blocks, the storey fragilities practically coincide, while the "ground" fragilities differ considerably from those of the four stories. In principle, the fragility curves should coincide since they provide a property of the system that should not be sensitive to the ground motion set. However, due to the substantially different frequency content of the ground motions this in not the case here. Of interest is also to show the fragilities obtained using as $IM^{(b)}$ the PGV (or PFV) instead of the PGA (Fig. 8). Adopting the PGV, the storey fragilities appear more dispersed compared to the $PFA/gtan\alpha$, which is more profound for the stocky block. Quantitatively, as before, the stocky block is more vulnerable on the ground, while the slender block is less affected by the structure compared Figure 5a. As a general conclusion, although qualitatively our conclusions are not affected by the $IM^{(b)}$, the fragility curves will differ and their interpretation requires attention. Furthermore, Figures 7a and 8a show the 90% confidence intervals which again verify the statistical significance of the fragilities obtained.

In order to calculate the limit-state mean annual frequencies (MAF) of the block, we adopt the hazard curve that corresponds to a site in the island of Crete, Greece. As discussed in a previous section, the limit-state MAFs are "exactly" calculated with Eq. 6. Alternatively, the MAFs can be calculated with Eq. 7 finding separately the fragility of the block and of the structure. The calculation of Eq. 7 requires the derivative of the block's fragility, which essentially is the probability density function (PDF) for a number of discrete limit-states. For the example considered, the MAFs of Eq. 6 and Eq. 7 are shown in Table 1 for the first and the fourth storey of the RC building considered. In Eq. 7 two $IM^{(b)}$ were considered, $PGA/gtan\alpha$ and PFV. Sufficient accuracy between the MAFs of the two approaches is achieved when the PFV is used as the intermediate variable in Eq. 7, while significant errors are observed for $IM^{(b)} = PFA/gtan\alpha$. Although not shown, poor results were observed when the PFA was

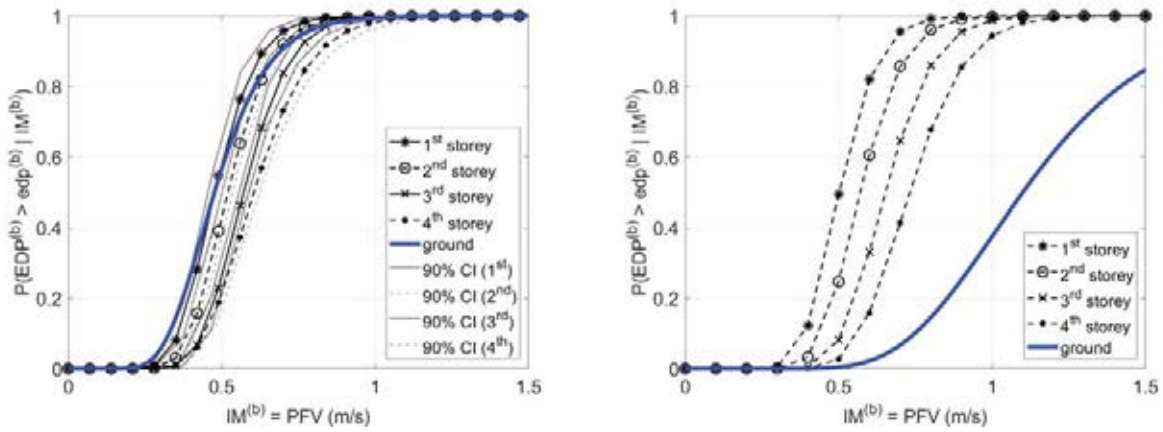

(a) (b)

Figure 8: Storey overturning fragility curves using PFV as the IM of the block: (a) slender block ($R = 1.0m, \alpha = 0.2$), (b) stocky block ($R = 1.0m, \alpha = 0.35$).

used as $IM^{(b)}$. Moreover, the simplified method of Eq. 7 produces slightly better estimates for the slender block. The cloud data should be handled carefully, since the associated dispersion is naturally large. The main reason for the large variation of the MAFs in Table 1 is the biased fragilities of the blocks when the IM considered is the PFA. However, we have observed that using the PFV as IM, the approximate evaluation tends to produce smaller errors.

Table 1: Limit-state MAFs obtained for a rocking block using the exact (Eq. 6) and the simplified approach (Eq. 7) with either $PFA/gtan\alpha$ or PFV as the intermediate variables.

Slender block				
storey	$IM^{(b)}$	$(\theta/\alpha \leq 0.3)$	$(\theta/\alpha \leq 0.5)$	$(\theta/\alpha \leq 1.0)$
1^{st} storey	exact	7.389 $\times 10^{-4}$	2.918 $\times 10^{-4}$	1.894 $\times 10^{-4}$
	simpl. PFA	13.304 $\times 10^{-4}$	6.843 $\times 10^{-4}$	5.760 $\times 10^{-4}$
	simpl. PFV	5.470 $\times 10^{-4}$	2.427 $\times 10^{-4}$	1.940 $\times 10^{-4}$
4^{th} storey	exact	58.502 $\times 10^{-4}$	12.372 $\times 10^{-4}$	4.035 $\times 10^{-4}$
	simpl. PFA	40.966$\times 10^{-4}$	21.168 $\times 10^{-4}$	12.938 $\times 10^{-4}$
	simpl. PFV	33.753 $\times 10^{-4}$	11.930 $\times 10^{-4}$	4.959 $\times 10^{-4}$
Stocky block				
storey	$IM^{(b)}$	$(\theta/\alpha \leq 0.1)$	$(\theta/\alpha \leq 0.3)$	$(\theta/\alpha \leq 1.0)$
1^{st} storey	exact	3.328 $\times 10^{-4}$	1.831 $\times 10^{-4}$	1.661 $\times 10^{-4}$
	simpl. PFA	5.556 $\times 10^{-4}$	4.534 $\times 10^{-4}$	4.395 $\times 10^{-4}$
	simpl. PFV	2.753 $\times 10^{-4}$	1.903 $\times 10^{-4}$	1.822 $\times 10^{-4}$
4^{th} storey	exact	53.987 $\times 10^{-4}$	7.115 $\times 10^{-4}$	1.661 $\times 10^{-4}$
	simpl. PFA	30.435$\times 10^{-4}$	11.557 $\times 10^{-4}$	6.623 $\times 10^{-4}$
	simpl. PFV	31.043 $\times 10^{-4}$	6.180 $\times 10^{-4}$	2.269 $\times 10^{-4}$

The comparison of the MAF estimates is better understood looking at the fragilities of Figure 9. The fragility $P(EDP^{(b)}|IM^{(s)})$ is compared with the direct calculation and is calculated as $P(EDP^{(b)}|IM^{s}) = \int_{IM^{(b)}} P(EDP^{(b)}|IM^{(b)})\, dP(IM^{(b)}|IM^{(s)})$. Essentially the calculation

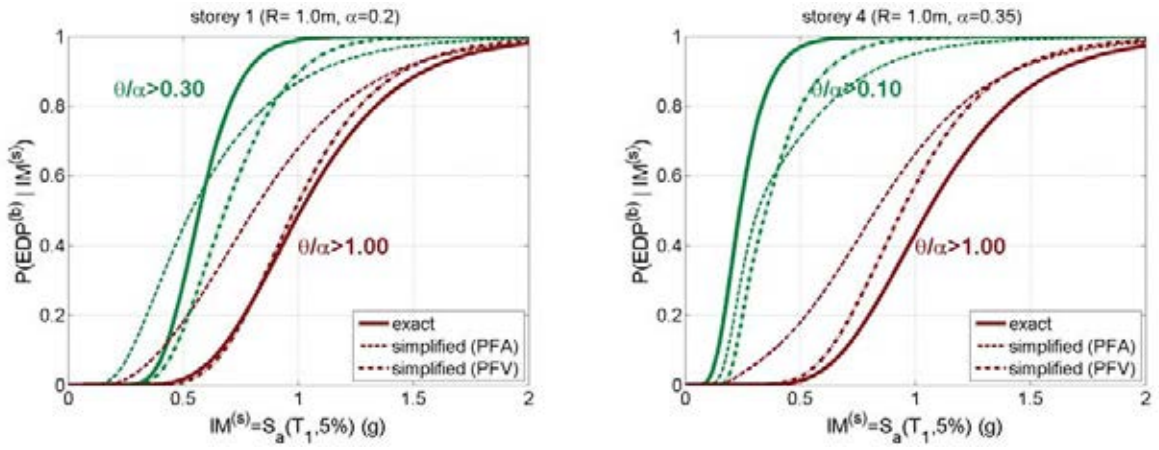

(a) (b)

Figure 9: Fragility curves using the exact (Eq. 6) and the simplified approach (Eq. 7) for the slender block ($R = 1.0m, \alpha = 0.2$) and the stocky block ($R = 1.0m, \alpha = 0.35$): (a) first storey, (b) forth storey, respectively.

of Eq. 7 is repeated leaving out the slope of the hazard curve $d\lambda_{IM^{(s)}}$, which is common for both MAF equations. Figure 9 shows the good performance of PFV as opposed to $PFA/gtan\alpha$, while better agreement is shown for the overturning limit-state and for the slender block.

Accepting that the choice of the $IM^{(b)}$ is important, it is necessary to investigate where do the errors shown in Figure 9 come from. This is understood comparing Figure 7 and Figure 9. Figure 7 shows that the fragility curves of the block at the building and at the ground will differ for the stocky block but not for the slender block. Since the collapse of the building does not affect the overturning fragility of the slender block (Fig. 7a), the overturning fragility of the slender block is almost the same regardless, if the structure's collapse is neglected or not, hence the overturning MAF of Figure 9 is closely estimated. On the other hand, for the slender block, the building and the ground fragilities differ and this is transfered to Figure 9b. However, even for the stocky block, the solution provided is acceptable given the many sources of uncertainty on the problem at hand. Another important remark is that the block used in this example were obtained including the building's collapse. Therefore, when the building's collapse does affect the fragilities, as in the case of the slender block, Eq. 7 is accurate. This hampers the use of Eq. 7 when generic fragility curves are to be adopted.

7 CONCLUSIONS

The fragility assessment of freestanding building contents has been discussed. The building contents were modelled as rigid blocks and it was assumed that they are hosted in a four-storey RC building. It has been shown that the problem addressed is complicated since the response of the structure and the contents are coupled. The findings of the study have been been obtained using a single two-dimensional, four-storey building and hence cannot be always generalized. For this reason, further research is required in order to fully understand the effect of the structure on the fragility of freestanding contents. Nevertheless, the work presented should be considered as an attempt to offer some first guidelines on how the rocking problem can be handled for freestanding objects that are hosted in a building.

REFERENCES

[1] G.W. Housner, The behavior of inverted pendulum structures during earthquakes. *Bulletin of the Seismological Society of America*, **53(2)**, 404–417, 1963.

[2] M. Fragiadakis, S. Diamantopoulos, Fragility and risk assessment of freestanding building contents. *Earthq Eng Struct Dyn*, **49(10)**, 1028–1048, 2020.

[3] S. Diamantopoulos, M. Fragiadakis, Seismic response assessment of rocking systems using single degree-of-freedom oscillators. *Earthq Eng Struct Dyn*, **48(7)**, 689–708, 2019.

[4] Y. Ishiyama, Motions of rigid bodies and criteria for overturning by earthquake excitations. *Earthq Eng Struct Dyn*, **10**, 635–650, 1982.

[5] E.G. Dimitrakopoulos, A.I Giouvanidis, Seismic response analysis of the planar rocking frame. *Journal of Engineering Mechanics*, **141(7)**, 04015003, 2015.

[6] EG. Dimitrakopoulos, TS. Paraskeva, Dimensionless fragility curves for rocking response to near-fault excitations. *Earthq. Eng. Struct. Dyn*, **44(12)**, 2015–2033, 2015.

[7] I. Psycharis, M. Fragiadakis, I. Stefanou, Seismic reliability assessment of classical columns subjected to near-fault ground motions. *Earthq. Eng. Struct. Dyn*, **42(14)**, 2061–2079, 2013.

[8] I. Kavvadias, L. Vasiliadis, Ar. Elenas, Seismic Response Parametric Study of Ancient Rocking Columns. *International Journal of Architectural Heritage*, **11(6)**, 791–804, 2017.

[9] K. Porter, K. Farokhnia, D. Vamvatsikos, I. Cho, *Guidelines for component-based analytical vulnerability assessment of buildings and nonstructural elements*. Technical Report, 2015.

[10] M. Fragiadakis, D. Vamvatsikos, M.G. Karlaftis, N.D. Lagaros, M. Papadrakakis, Seismic assessment of structures and lifelines. *Journal of Sound and Vibration*, **334**, 29–56, 2015.

[11] FEMA, *FEMA P-58-1: Seismic Performance Assessment of Buildings - Volume 1, Methodology elements*. 2012.

[12] F. Jalayer, *Direct probabilistic seismic analysis: Implementing non-linear dynamic assessments*. Department of Civil and Environmental Engineering, Stanford University, CA, 2003.

[13] JW. Baker, Efficient Analytical Fragility Function Fitting Using Dynamic Structural Analysis. *Earthquake Spectra*, **31(1)**, 579–599, 2015.

[14] D. Vamvatsikos, M. Fragiadakis Incremental dynamic analysis for estimating seismic performance sensitivity and uncertainty. *Earthq.Eng. Struct. Dyn*, **39(2)**, 141–163, 2010.

[15] J.W. Baker, Efficient analytical fragility function fitting using dynamic structural analysis. *Earthq Spectra*, **31(1)**, 579–599, 2015.